J Electroceram (2006) 16:477–481
DOI 10.1007/s10832-006-9901-5

Ferroelectric properties of $(Bi_{3.15}Nd_{0.85})Ti_3O_{12}$ with decreasing film thickness

Xingsen Gao · John Wang

Abstract Film texture and ferroelectric behaviors of $(Bi_{3.15}Nd_{0.85})Ti_3O_{12}$ (BNdT) of layered-perovskite structure deposited on $Pt/TiO_2/Si$ substrate are dependent on the film thickness. When the film thickness is reduced from ∼240 to ∼120 nm, BNdT grains evolve from a rod-like morphology to a spherical morphology, accompanied by a decrease in average grain size. At the same time, *P-E* hysteresis transforms from a square-shaped hysteresis loop ($2Pr \sim 24.1\ \mu C/cm^2$ at 240 nm) to a relative slimmer hysteresis loop (with a lower $2Pr = 19.8\ \mu C/cm^2$ at 120 nm). The nonvolatile polarization (ΔP) shows a maximum at the film thickness of 160 nm, where ΔP was measured to be 14.7 $\mu C/cm^2$ and 6.8 $\mu C/cm^2$ at 5 V and 3 V, respectively. A small amount of excess bismuth in the film thickness of 130 nm, introduced by co-sputtering, can lead to a much enhanced remanent polarization ($2Pr$ of 21.3 $\mu C/cm^2$ at 5 V and 15.2 $\mu C/cm^2$at 3 V), which is promising for low voltage FRAM applications.

Keywords $Bi_4Ti_3O_{12}$ thin film · Ferroelectric behaviors · Thickness dependence · Layered perovskite structure · FRAM

1 Introduction

For the past several years, there has been a surge of interest in investigation into $(Bi,Nd)Ti_3O_{12}$ (BNdT) thin films, because of their lead-free composition and excellent polarization behaviors, which make them promising for applications in random access memory (FRAM), sensor, actuator and microelectromechanical systems (MEMS) [1–3]. In comparison to the widely used $Pb(Zr,Ti)O_3$(PZT) and $SrBi_2Ta_2O_9$ (SBT) for FRAM, Nd-doped $Bi_4Ti_3O_{12}$ exhibits a combination of high fatigue resistance, retention of nonvolatile polarization, together with a relatively lower processing temperature [2–5]. Several deposition techniques, including sol-gel [4–6], pulsed laser deposition (PLD) [7, 8], metalorganic chemical vapor deposition (MOCVD) [9], and RF sputtering, have been employed to synthesize Nd_2O_3-doped $Bi_4Ti_3O_{12}$ (NBdT) based thin films [10].

To understand the ferroelectric thin films towards the nanometer scale, there has been attempt to refine the film thickness, which indeed has led to several unique phenomena in their ferroelectric behaviors [11–13]. Realization of improved electrical properties at reduced film thickness is of considerable interest, as the thin film and device technologies are driving towards miniaturization, for example for small cell size and low operating polarization voltage of FRAM (at 3 V or 5 V) [14]. Therefore, the main objective of this work is to investigate the texture and ferroelectric behaviors of BNdT with decreasing film thickness. For this, BNdT films of varying thickness in the range of 120 to 240 nm are deposited by RF sputtering on $Pt/TiO_2/Si$.

2 Experimental procedures

BNdT thin films of varying thicknesses were deposited by RF magnetron sputtering on $Pt/TiO_2/Si(100)$ substrates from a two-inch ceramic target of single phase $(Bi_{3.15}Nd_{0.85})Ti_3O_{12}$ synthesized by solid-state reaction with 5 mol% Bi_2O_3 excess. For selected film thicknesses, a small amount of excess bismuth was introduced by co-sputtering, from two-inch bismuth oxide target. The deposition ambient was pure Ar gas controlled in the pressure range of 10–15 mTorr. The RF

X. S. Gao · J. Wang (✉)
Department of Materials Science and Engineering, Faculty of Engineering, National University of Singapore, Singapore 117576
e-mail: msewangj@nus.edu.sg

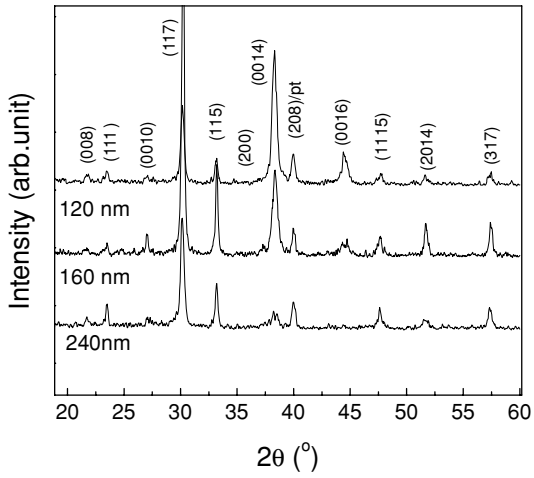

Fig. 1 X-ray diffraction patterns for BNdT of three film thicknesses, namely 120, 160 and 240 nm, respectively, deposited by RF sputtering at room temperature and then annealed at 700°C for 5 min

power employed was in the range of 120–160 W. BNdT films of required thicknesses were deposited at room temperature, followed by a rapid thermal annealing in oxygen at 700°C for 5 min.

Phases and textures of the BNdT thin films were examined by using an X-ray diffractionmetry (XRD, CuK_{α}). Scanning electron microscopy (SEM, Philips, XL 30) and atomic force microscopy (AFM, Digital instruments) were used to study their surface morphologies. Their thicknesses were measured by using an optical Filmetric thinness analyzer (Filmetrics Inc., USA; reflective mode) and SEM cross-section images. An impedance gain phase analyzer (Solatron 1261) was utilized to characterize their dielectric properties and ac conductivity. A Radiant precise workstation (Radiant Technologies) was employed to measure their ferroelectric and fatigue properties. Prior to these electrical characterizations, gold electrodes with areas of 0.31×10^{-4} cm^2 were coated by dc sputtering through a shadow mask.

3 Results and discussion

Figure 1 shows XRD spectra for BNdT films with three film thicknesses of 120, 160 and 240 nm, respectively, that were annealed at 700°C for 5 min. All the BNdT thin films were deposited by RF sputtering at room temperature, followed by rapid thermal annealing. They all show wanted layered-perovskite structures, and no apparent impurity phases being detected.

Surface morphologies of the three BNdT films, which were examined by AFM, are shown in Fig. 2. BNdT thin film of 240 nm in thickness shows a rod-like grain morphology, together with a small amount of spherical-shaped, small grains. A similar rod-like morphology was observed in the

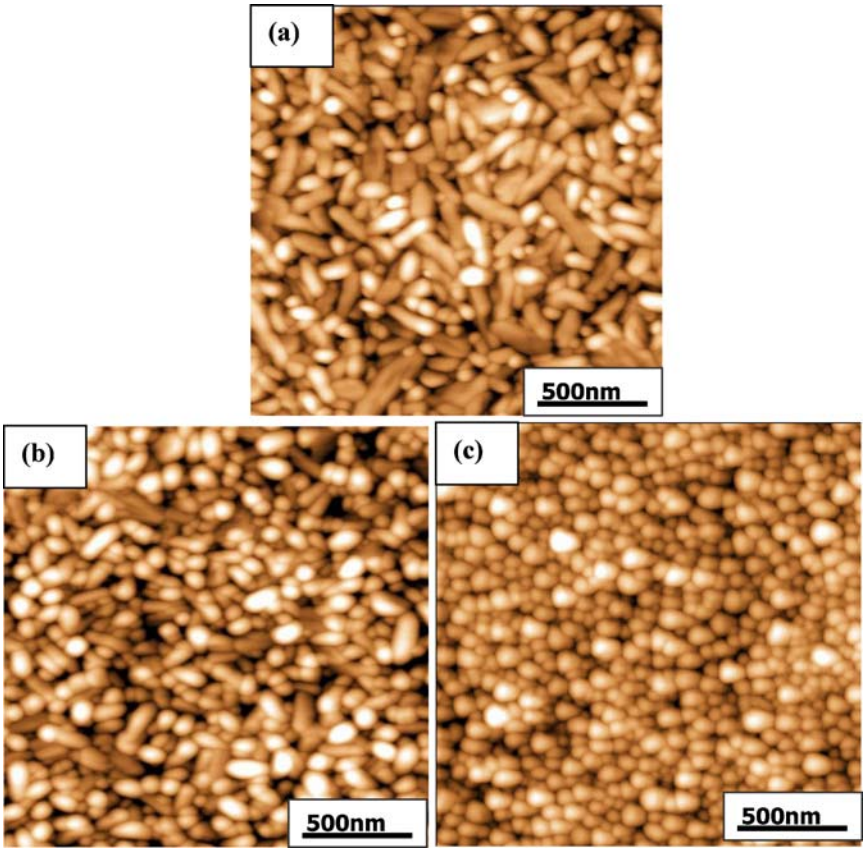

Fig. 2 AFM surface morphologies for the BNdT films of three film thicknesses: (a) 240, (b) 160 nm, and (c) 120 nm, deposited by RF sputtering at room temperature and annealed at 700°C for 5 min

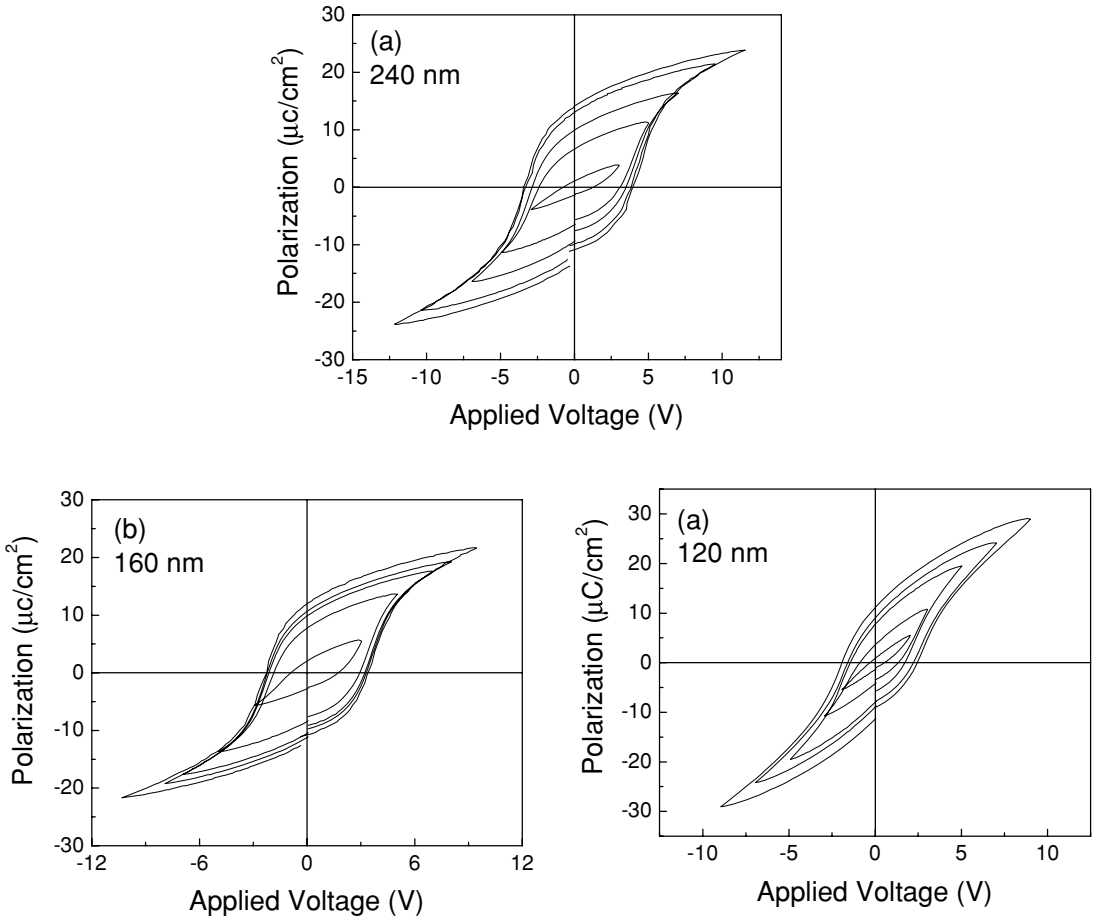

Fig. 3 P-E hysteresis loops for the BNdT films with three different thicknesses deposited by RF sputtering at room temperature and annealed at 700°C for 5 min

film thickness of 160 nm, although there is an apparent reduction in grain size and aspect ratio of the rod-like grains. Further decrease in film thickness to 120 nm leads to a significant change in grain morphology and size, where spherical grain morphology is resulted, and the average grain size is of ∼70 nm. This shows that the grain growth of BNdT is greatly affected by the film thickness. A thinner film thickness suppresses the grain growth of BNdT films at the thermal anneal temperature.

Figure 3(a) plots the hysteresis loops for the three BNdT thin films measured at different applied voltages. Well established square-shaped hysteresis loops are shown for the BNdTs of both 240 nm and 160 nm in thickness. In particular, the film of 240 nm thickness exhibits a considerable higher $2Pr$ of $\sim 24\,\mu C/cm^2$ and a coercive field of 151 kV/cm, as comparable to the randomly orientated BNdT film prepared by other methods [8, 9]. A similar polarization loop is shown for the film of 160 nm thickness, although there is a slight increase in coercive filed, which is related to the blocking layer that has been commonly observed in ferroelectric films [11, 13]. In comparison, there is an obvious change in polarization loop for the BNdT of 120 nm in thickness, where a much slimmer *P-E* hystereis loop is observed. It also exhibits an unsaturated characteristic, even at a rather high applied voltage, where there is also a reduction in remanent polarization ($2Pr$ of 19.8 $\mu C/cm^2$), indicating a degradation in ferroelectricity.

To further demonstrate the change in ferroelectricity of the BNdT thin film against film thickness, the polarization and coercive field as a function of electric field are plotted in Fig. 4, for the three film thicknesses. They each demonstrate a gradual increase in remanent polarization with the rise in applied electrical field, before approaching the stability with further increase in electrical field. This is apparently due to the polarization saturation at a high enough electrical field (Fig. 4(a)). Under a given applied electrical field, the film thickness of 240 nm gives rise to the largest remenant polarization. In contrast, the BNdT film of 120 nm exhibit the smallest polarization, and it does not show a clear polarization saturation behavior, as shown in Fig. 3. Fig. 4(b) plots the coercive field as a function of applied electrical field for the three film thicknesses. Similar to the polarization behaviors, the coercive fields for the film thicknesses of 160 nm and 240 nm demonstrate a monotonous increase with rising

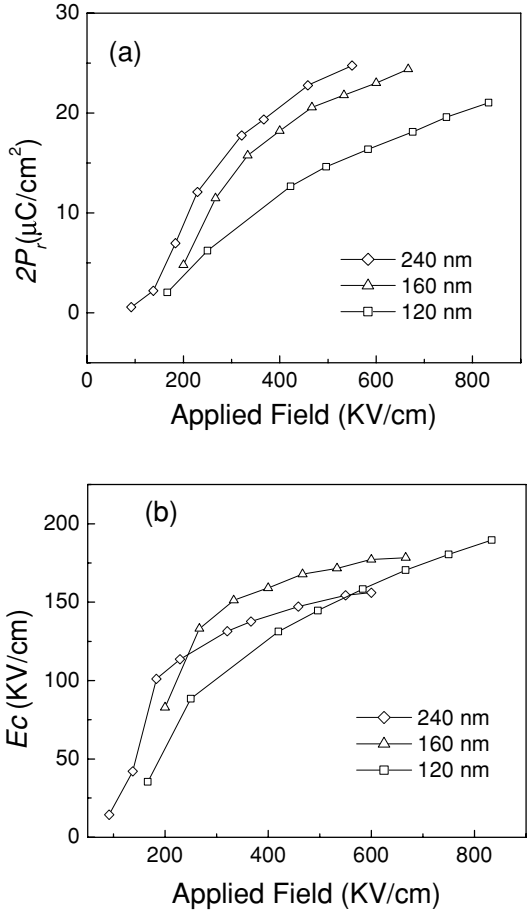

Fig. 4 Remanent polarization (a) and coercive field (b) as a function of applied electrical field for the BNdT films of three different thicknesses

applied electrical field. The former shows a higher coercive field at high applied electrical field, as can be accounted for by the existence of a non-ferroelectric blocking layer. In comparison, the film thickness of 120 nm exhibits a generally lower coercivity, and it does not show an obvious saturation with increasing electrical field.

For FRAM applications, one is concerned with the signal sensing margin for each operation voltage, which can be quantified by nonvolatile polarization ($\Delta P = P_{sw} - P_{ns}$, where P_{sw} is switching polarization, and P_{ns} is non-switching polarization). The nonvolatile polarization for the three film thicknesses at both operation voltages of 3 V and 5 V are listed in Table 1, where the film thickness of 160 nm apparently shows the highest non-volatile polarization (ΔP) of

Table 1 Nonvolatile polarization (ΔP) measured at 3 V and 5 V for the three BNdT films of different thicknesses

Nonvolatile polarization	220 nm	160 nm	120 nm
ΔP at 3 V ($\mu C/cm^2$)	2.6	6.8	6.4
ΔP at 5 V ($\mu C/cm^2$)	13.1	14.7	12.9

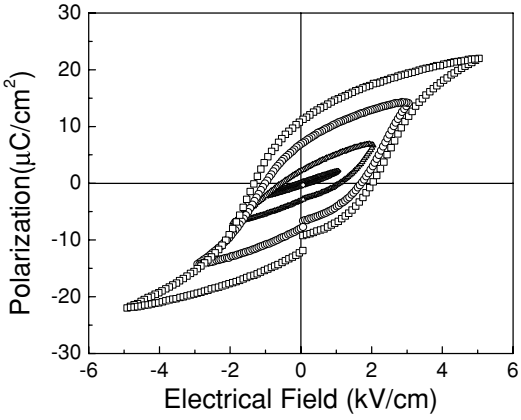

Fig. 5 *P-E* hysteresis for the BNdT film of 120 nm in thickness, when compensated by a small amount of excess bismuth oxide, through co-sputtering, showing the much improved polarization behavior

14.7 $\mu C/cm^2$ and 6.8 $\mu C/cm^2$ at 5 V and 3 V, respectively. Both film thicknesses of 120 and 240 nm give rise to a reduction in the polarization. At 3 V, the polarization value is too small to be useful for memory devices. Therefore, too low a film thickness fails to enhance the polarization at low operation voltage, due to the loss in ferroelectricity.

As shown in Figs. 2 and 3, the film thickness of 120 nm gives rise to small, sphere grain morphology together with lowered polarization, suggesting a correlation between the refined grain size and poor ferroelectric behaviors. To facilitate grain growth, a small amount of excess bismuth was introduced by a co-sputtering using a bismuth oxide target. As expected, the ferroelectric behaviors are significantly enhanced by the compensation of bismuth oxide. As shown in Fig. 5, a well saturated hysteresis is obtained at the test voltage above 3 V for the BNdT film, where the remament polarization of *2Pr* is measured to be 15.2 and 21.3 $\mu C/cm^2$ at 3 V and 5 V, respectively. Therefore, the compensation of a small amount of bismuth oxide in BNdT thin films of refined film thickness can lead to the wanted improvement in electrical properties.

4 Conclusions

Bismuth based BNdT films of varying film thicknesses, deposited on $Pt/TiO_2/Si$ substrates by RF sputtering, were studied for texture development and ferroelectric behaviors. A rod-like grain morphology is observed for film thickness of 240 and 160 nm. In contrast, smaller spherical-shaped grains are shown for the film thickness of 120 nm. The former two demonstrate a well established *P-E* hysteresis loop with a remanent polarization *2Pr* of ~24 $\mu C/cm^2$. In contrast, the film thickness of 120 nm gives rise to a much slimmer loop with low polarization of 19.8 $\mu C/cm^2$, which is unsaturated. A non-volatile polarization of 6.8 and 14.7 $\mu C/cm^2$

is measured for the BNdT film of 160 nm in thickness at 3 V and 5V respectively. On the one hand, too thin a film thickness (e.g., 120 nm) leads to degradation in ferroelectrictity of the thin film. On the other hand, when compensated by a small amount of excess bismuth, a much improved ferroelectric behavior is observed for the film thickness of 130 nm, where the remanent polarizations $2Pr$ are 15.2 and 21.3 μC/cm^2 at 3 V and 5 V, respectively.

Acknowledgments This paper is based upon work supported by the Science and Engineering Research Council—A*Star, Singapore, under Grant No.: 022 107 0007. Authors acknowledge the support of the National University of Singapore.

References

1. B.H. Park, B.S. Kang, S.D. Bu, T.W. Noh, J. Lee, and W. Jo, *Nature*, **401**, 682 (2002).
2. U. Chon, H.M. Jang, M.K. Kim, and C.H. Chang, *Phys. Rev. Lett.*, **89**, 0876011 (2002).
3. C. A-Paz de Araujo, J.D. Cuchiaro, L.D. McMillian, M.C. Scott, and J.F. Scott, *Nature*, **374**, 627 (1995).
4. H. Uchida, H. Yoshikawa, I. Okada, H. Matsuda, T. Lijima, T. Watanabe, T. Kojima, and H. Fubakubo, *Appl. Phys. Lett.*, **81**, 2229 (2002).
5. D. Wu, Y.D. Xia, A.D. Li, Z.G. Liu, and N.B. Ming, *J. Appl. Phys.*, **94** 7376 (2003).
6. H. Uchida, H. Yoshikawa, I. Okada, H. Matsuda, I. Takashi, T. Watanabe, and H. Funakubo, *Jpn. J. Appl. Phys. Lett.*, **41**, 6820 (2002).
7. S.T. Zhang, X.J. Zhang, H.W. Cheng, Y.F. Chen, Z.G. Liu, N.B. Ming, X.B.Hu, and J.Y. Wang, *Appl. Phys. Lett.*, **83**, 4378 (2003).
8. A. Gang, Z.H. Barber, M. Dawber, J.F. Scott, A. Snedden, and P. Lightfoot, *Appl. Phys. Lett.*, **83**, 2415 (2003).
9. T. Kojima, T. Sakai, T. Watanabe, H. Funakubo, K. Saito, and M. Osada, *Appl. Phys. Lett.*, **81**, 2746 (2002).
10. X.S. Gao, J.M. Xue, and J. Wang, *J. Appl. Phys.*, **97**, 034101 (2005).
11. V. Nagarajan, I.G. Jenkins, S.P. Alpay, H. Li, S. Aggarwal, L. Salamanca-Riba, L. Roytburd, and R. Ramesh, *Appl. Phys. Lett.*, **86**, 595 (1999).
12. K.T. Li and V.C. Lo, *Solid State Comm.*, **132**, 49 (2004).
13. D. Wu, A.D. Li, H.Q. Ling, T. Yu, Z.G. Liu, and N.B. Ming, *J. Appl. Phys.*, **87**, 1795 (2000).
14. T. Oikawa, H. Morioka, A. Nagai, H. Funakubo, and K. Saito, *Appl. Phys. Lett.*, **85**, 1756 (2004).